Testing the redox theory of aging under parasitism

Luís M. Silva [1, 2, 3 *], Alessandro Belli [1, 3], Jacob C. Koella [1]

[1] Institute of Biology, University of Neuchâtel, Neuchâtel, Switzerland

[2] Department of Zoology, University of British Columbia, Vancouver, Canada

[3] These authors contributed equally.

* Corresponding author: luis.silva@ubc.ca (LMS)

ORCID: 0000-0002-8203-4006 (LMS)

Abstract

The redox theory of aging proposes that an oxidative imbalance, possibly amplified by infection, drives senescence. We experimentally evolved mosquitoes under early or late reproduction with or without parasite exposure, and quantified longevity, fecundity, and redox markers. Although selection generated the expected life-history divergence, there was only a poor non-linear association between a redox gradient and longevity. Thus, oxidative stress contributed to, but did not determine, the evolution of aging.

Introduction

Aging evolves because the force of natural selection declines with age [1–4], allowing late-acting deleterious effects to accumulate [5]. As a consequence, evolutionary theories, such as the *selective shadow* (or antagonistic pleiotropy) and the *disposable soma hypothesis* [2,5,6], predict a trade-off between investing in early reproduction and maintaining somatic function later in life. Under this framework, Rose and colleagues (and subsequent research groups) demonstrated that selection for early reproduction should favour high fecundity at the expense of longevity [7–9].

The physiological mechanisms, however, through which these life history trade-offs shape aging remain under active debate [10,11]. One well-known hypothesis is the *redox theory of aging* (RTA) [12]. The latter proposes that age-related decline results from shifts in the balance between reactive oxygen species (ROS), antioxidant defences, and cellular repair. Therefore, life-history traits associated with high reproductive effort or chronic immune activation should push organisms toward more oxidized physiological states, and life histories that favour late reproduction should promote stronger antioxidant capacity. However, empirical tests that explicitly link long-term selection on life history with changes in oxidative physiology and aging are rare.

Complicating these ideas, organisms in nature face frequent and even chronic immune challenges that affect reproductive investment, metabolic allocation, and redox processes [13–15] and thus shape how aging evolves. Infection is often expected to accelerate physiological decline, either through direct pathology (immunopathology) [16], oxidative immune responses (*e.g.,* ROS and inflammaging) [17], or energetic diversion away from somatic maintenance. Yet, hosts can also adopt alternative strategies, such as disease tolerance [18], that mitigate fitness costs without reducing the parasite burden. Whether parasitism restructures redox physiology or interacts with life-history evolution to alter aging remains largely unresolved.

Hence, we set out to test the RTA in a mosquito-microsporidian system. In particular, we examined whether the pressure of parasitism disrupts the redox balance and its evolution. We experimentally selected *Aedes aegypti* females to reproduce either early (7–14 days after emergence) or late (35–42

days) either with or without exposure to their natural microsporidian parasite, *Vavraia culicis* [19], which triggers oxidative immune responses [13]. After at least ten generations, we quantified how selection on reproduction and parasitism shaped life history **(Fig. 1)** and redox expression **(Fig. 2)**. More broadly, we asked whether the RTA can be applied to ecological and epidemiological settings, where hosts are continually exposed to parasites and must navigate the inherent trade-offs that shape the evolution of aging.

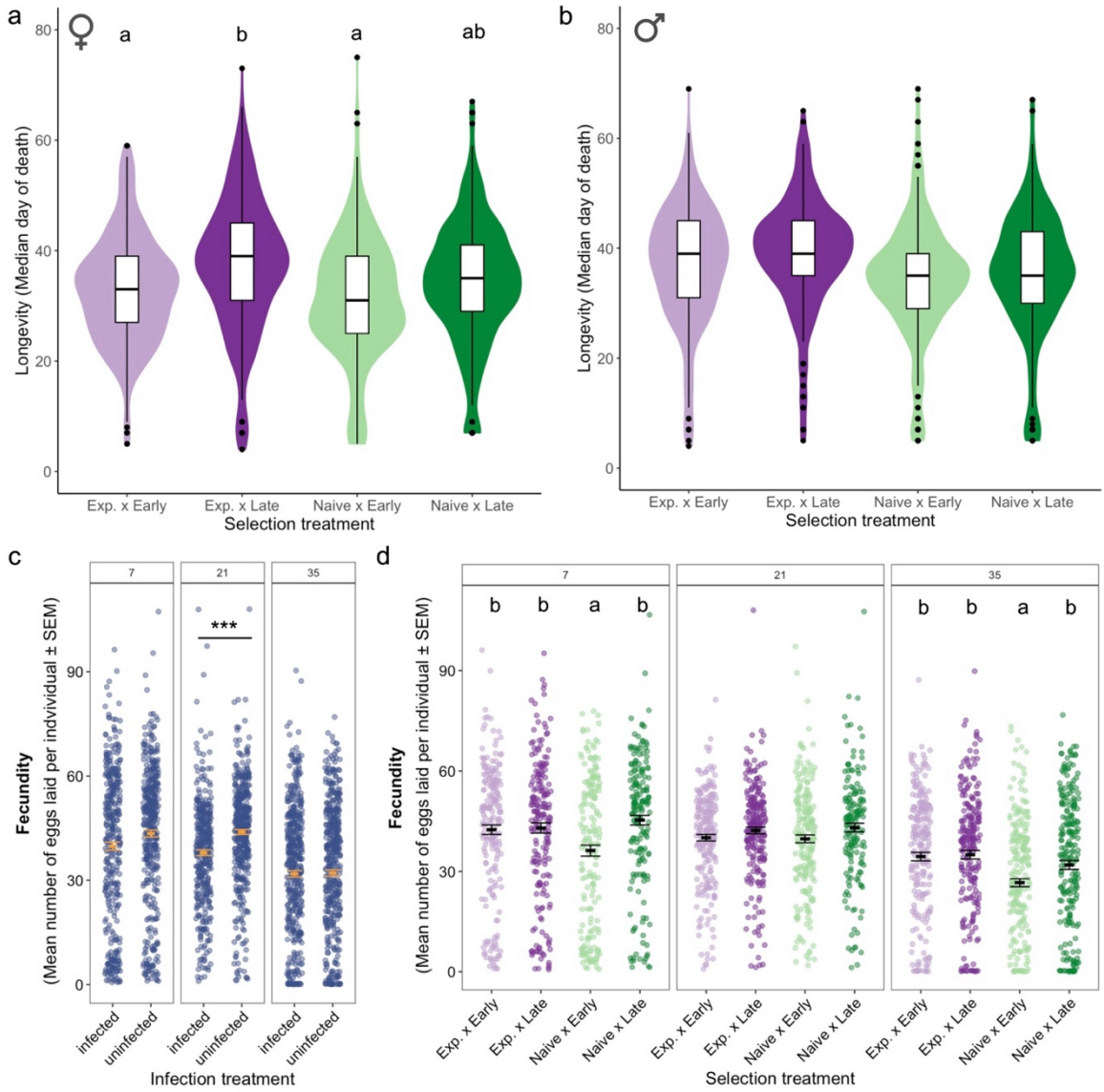

Figure 1. Evolution of longevity and fecundity across selection treatments. Median longevity of female **(a)** and male **(b)** mosquitoes after 10 generations of selection for early or late reproduction, with or without exposure to the parasite *V. culicis*. Sample sizes were: 315 females and 284 males in Exposed and Early; 308 females and 287 males in Exposed and Late; 281 females and 274 males in Naive and Early; and 295 females and 300 males in Naive and Late. Effect of **(c)** infection and **(d)** selection on fecundity, measured at three ages (7, 21 and 35 days after emergence). Each point is an individual, and

the black bars show means and the respective standard errors. Asterisks (***) indicate a significant difference, with a *p*-value of < 0.001, whereas letters denote results of post-hoc multiple comparisons tests conducted after the respective GLMM. Absence of letters indicates no difference between treatments, according to the multiple comparisons test. Sample sizes for the fecundity assay in the presence or absence of infection were 359 and 404 females at day 7, 371 and 442 at day 21, and 470 and 471 at day 35, respectively. Across selection treatments, sample sizes at day 7 were 203 (Exposed–Early), 194 (Exposed–Late), 184 (Naive–Early), and 182 (Naive–Late); at day 21 they were 223, 222, 205, and 153; and at day 35 they were 237, 232, 233, and 239, respectively.

Results

Experimental evolution **(Supplementary Fig. 1)** generated a divergence in aging and reproduction among the four selection regimes **(Fig. 1)**. Females selected for late reproduction lived significantly longer than those selected for early reproduction ($\chi^2 = 20.62$, $df = 1$, $p < 0.001$; **Fig. 1a**), but males did not **(Fig. 1b),** as expected from evolutionary predictions. Parasite exposure increased host longevity in both sexes (Females: $\chi^2 = 1.29$, $df = 1$, $p = 0.005$; Males: $\chi^2 = 1.29$, $df = 1$, $p = 0.040$; **Fig. 1; Supplementary Table 1**). However, upon the death of the mosquitoes, selection treatments did not differ in the proportion of clearance or in the parasite load **(Supplementary Fig. 2)**. In other words, exposed hosts evolved higher disease tolerance (or fitness overcompensation), as they live longer (higher fitness) in the absence of infection, but not higher parasite resistance, as there was no evidence of stronger clearance.

We quantified five markers of redox balance: malondialdehyde (MDA) as a measure of oxidative damage; superoxide dismutase (SOD) as an indicator of antioxidant activity; and the glutathione ratio and its components (GSH and GSSG) as markers of oxidative balance. Among these, only MDA showed a marginal interaction between reproductive regime and parasite exposure ($\chi^2 = 4.63$, $df = 1$, $p = 0.031$; **Fig. 2a; Supplementary Fig. 3**). Oxidative damage differed subtly across treatments, with parasite exposure slightly increasing MDA levels in early-reproducing lines but not in late-reproducing lines. This interaction was weak and highly overlapping among groups, indicating that neither factor produced strong or consistent divergence on its own. Overall, although parasitism modestly modulated MDA depending on reproductive regime ($\chi^2 = 5.17$, $df = 1$, $p = 0.023$), the evolved lines exhibited broadly similar oxidative damage profiles across treatments **(Fig. 2a)**.

Nevertheless, we observed significant variation in the redox markers. Hence, to summarize covariation among markers, we performed a principal component analysis (PCA) on replicate-level means. PC1 explained 39% of the variance and captured an oxidative–reductive gradient: higher scores reflected more oxidized profiles with elevated MDA, GSSG and GSH:GSSG ratio, whereas lower scores reflected more reduced profiles with higher GSH and SOD **(Fig. 2b, Supplementary Tables 3 and 4)**. PC2 explained a further 33% of the variance and represented residual differences among markers. Lines

selected for early reproduction, especially under parasite exposure, tended to occupy the more oxidized end of PC1, while late-selected lines were generally more reduced. However, all four selection regimes still overlapped in redox space, indicating that evolutionary responses in oxidative physiology were modest and heterogeneous.

We then asked whether these multivariate redox profiles were associated with evolved differences in aging. Across lines, PC1 scores explained a moderate fraction of the variation in median longevity of uninfected females **(Fig. 2c, Supplementary Table 5)**. A linear mixed model (LMM) indicated that more reduced profiles tended to be longer-lived. A generalized additive model (GAM) showed a weak but significant non-linear association between PC1 and median longevity (s(PC1): edf = 2.2, $F = 5.0$, $p = 0.026$), consistent with redox state explaining only a fraction of the among-line variation in lifespan. Thus, the baseline oxidative state was related to longevity, but not in the simple, canonical form often envisioned by the redox theory of aging. Overall, both univariate and multivariate analyses support a role for redox physiology in shaping aging; however, they also indicate that it only partially accounts for the substantial divergence in life histories generated by experimental evolution.

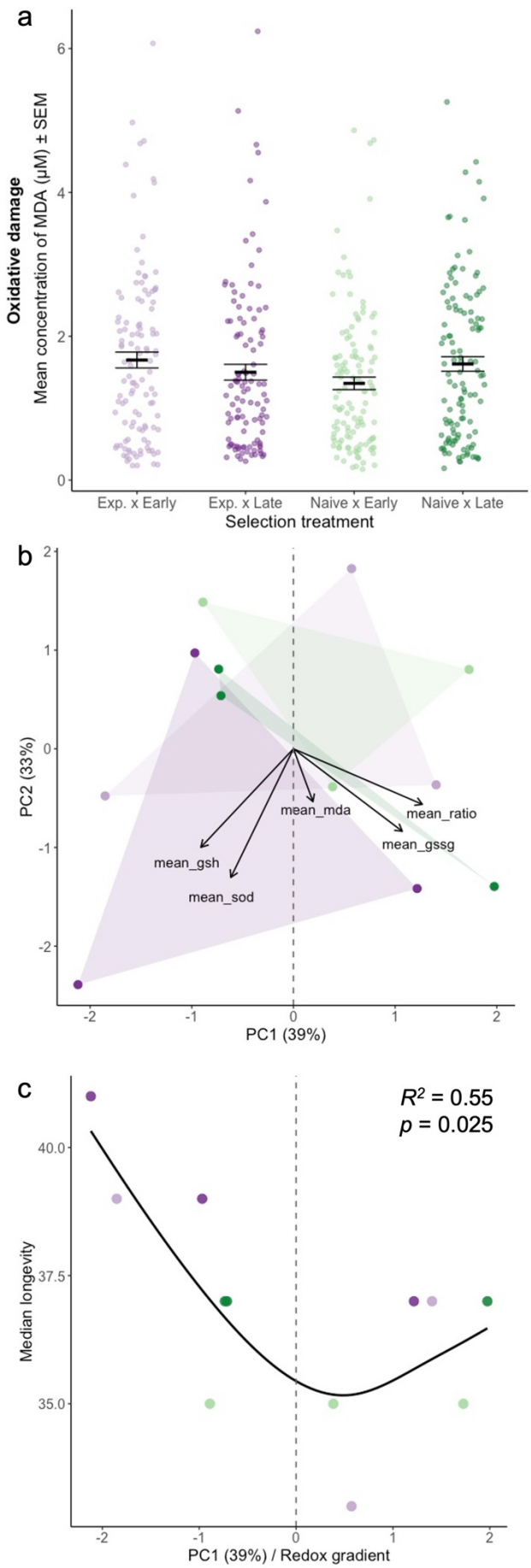
a
Oxidative damage
Mean concentration of MDA (µM) ± SEM
6
4
2
0
Exp. x Early
Exp. x Late
Naive x Early
Naive x Late
Selection treatment
b
PC2 (33%)
PC1 (39%)
mean_mda
mean_ratio
mean_gssg
mean_gsh
mean_sod
c
R^2 = 0.55
p = 0.025
Median longevity
40.0
37.5
35.0
PC1 (39%) / Redox gradient

Figure 2. Evolution of oxidative balance and aging. Oxidative balance of selected individuals was measured by assessing the concentrations of malondialdehyde (MDA - marker of oxidative damage), superoxide dismutase (SOD - marker of antioxidant activity), and individual values, as well as the ratio between oxidized and reduced glutathione (GSH: GSSG - marker of oxidative balance) without infection. **(a)** Only MDA was found to be affected by parasite- and reproduction-based selection (independently), although marginally and therefore not detectable in post hoc multiple comparisons tests. Sample size consisted of 117 "Exposed-Early", 109 "Late-Exposed", 122 "Naive-Early" and 120 "Naive-Late" females. **(b)** PCA of oxidative markers. PC1 (39% variance) captures a gradient from oxidized to reduced redox state. Negative loadings are associated with antioxidant capacity (GSH and SOD), whereas positive loadings are associated with oxidative damage (MDA, GSSG, and GSSG: GSH ratio). Arrows indicate marker loadings. **(c)** Relationship between redox PC1 and median adult longevity across replicates of the different selection treatments.

Discussion

Experimental evolution in our system revealed the life-history trade-offs predicted by theories of the evolution of senescence, but their mechanistic basis cannot be explained by the RTA alone. Selection for early reproduction resulted in short-lived and highly fecund mosquitoes, while selection for late reproduction extended their lifespan, consistent with evolutionary predictions of the selective shadow (or antagonistic pleiotropy) [5] and the disposable soma hypothesis [6]. Together, these findings highlight two key points: (i) aging cannot be solely explained by shifts in oxidative balance; and (ii) biology operates as an evolutionary game played on a life-history board [20], where aging emerges from strategic allocation between reproduction and somatic maintenance and traits [21]. Our data also aligns with principles described by Charlesworth (1994), which state that the tempo of aging is governed by the age-specific strength of selection, rather than simply by mechanistic deterioration[4]. Hence, aging responds to how selection is distributed across the life cycle, and to life-history trade-offs between reproduction, survival, and defence, rather than to damage accumulation alone.

The redox theory of aging provides a robust mechanistic framework by linking oxidative balance to age-related decline. In our experiment, however, redox physiology responded more weakly and less coherently than life history. Baseline oxidative markers differed only slightly among treatments, and the main multivariate redox axis (PC1) did not separate the four selection regimes. Nevertheless, lines at the more reduced end of the PC1-axis tended to live longer, whereas more oxidized or intermediate profiles were generally shorter-lived. The non-linear form of this relationship and the broad overlap among treatments in redox space suggest that a simple one-to-one link between oxidative state and the pace of aging is unlikely. Instead, they suggest that redox is one of several mechanistic pathways by which life-history evolution can influence senescence. This partial decoupling is consistent with critiques that oxidative biomarkers often fail to predict lifespan evolution across multiple taxa[22]. After all, ROS has been broadly recognized as functioning not only as damaging oxidants but also as integral signalling molecules regulating immunity, metabolism, and mitochondrial dynamics[23].

The effects of chronic exposure to parasitism further illustrate this complexity. Contrary to the expectation that infection accelerates physiological decline [24], parasite exposure increased longevity in both sexes. Evolving with parasites did not increase the ability to clear parasites or reduce parasite load. This pattern is consistent with evolutionary shifts in resource allocation and damage management, including changes in disease tolerance (the ability to mitigate infection-associated costs on host fitness) [18,25,26], rather than a straightforward enhancement of oxidative defences. Tolerance is expected to evolve when clearance is costly, ineffective, or the parasite does not pose a sufficient danger that necessitates its elimination [18]. Our parasite, *V. culicis*, causes relatively low virulence in mosquitoes, particularly in *A. aegypti* [27], although it still triggers an immune response from its hosts [28]. Hence, a low-virulence parasite, combined with constraints from early *versus* late reproduction, may favour disease tolerance rather than stronger resistance, particularly when resistance to this parasite already appears significant [27]. Allowing mosquitoes to evolve for many generations under these joint pressures, rather than relying on short-term manipulations or single-generation correlations, we capture this evolutionary realism. It reveals that redox leaves only a modest, context-dependent imprint, even when aging itself evolves strongly.

These findings have broader implications for the biology of aging. First, they emphasize that aging should be studied in a multidimensional space, which encompasses several traits regulated by interactions between metabolic allocation, immune activation, endocrine pathways, mitochondrial function, and even behavioural ecology. This multidimensionality reflects the "hallmarks of aging", which emphasize that molecular and physiological pathways (from nutrient sensing to mitochondrial dynamics) interact to shape lifespan [29]. Redox processes contribute to these dynamics, but they do not operate in isolation. Second, the evolution of tolerance in our system highlights how the expression of this specific strategy might be especially advantageous in the wild. An increase in tolerance in a host population is likely to be followed by a rise in the prevalence of the parasite [18], which is amplified by increases in disease transmission among infected tolerant hosts [30]. This has severe consequences for aging, as well as host-parasite coevolution and epidemiology.

Ultimately, our findings underscore the importance of integrating mechanistic aging research with an ecological and evolutionary perspective. Organisms rarely live in benign laboratory environments; instead, they face sustained immune challenges and fluctuating reproductive opportunities that shape the evolution of aging. Through the combination of experimental evolution with multivariate physiological analysis, we demonstrate that lifespan can evolve robustly even when canonical oxidative markers shift only slightly. A deeper understanding of how aging mechanisms intersect will be essential for predicting the evolution of aging and for designing evolutionarily informed approaches to promote healthy aging and improve age-specific responses to infection.

Materials and Methods

Experimental model

We used the microsporidian parasite *Vavraia culicis floridensis,* provided by James Becnel (USDA, Gainesville, FL) and the UGAL strain of the mosquito *Aedes aegypti* (obtained from Patrick Guérin, University of Neuchâtel). Mosquitoes were reared under standard laboratory conditions (26 ± 1ºC, 70 ± 5% relative humidity, and 12 h light/dark). *V. culicis* is a generalist, obligatory, intracellular parasite that infects mosquito epithelial gut cells. Mosquitoes are exposed to the microsporidian during the larval aquatic stage, where they ingest spores along with their food in the water. After replication within the larvae, as adults, they start producing spores from within the gut cells, re-infecting new cells and propagating the cycle until they kill the host. Spores are transmitted when infected individuals die in water or from mother to offspring by adhering to the surface of the eggs. Before starting the experiment, *V. culicis* was kept in large numbers, alternating every generation between infecting *A. aegypti* and *Anopheles gambiae* populations to ensure it remains a generalist parasite. The infection protocol was performed as described in detail in the experiments below, with two-day-old larvae being exposed to 10,000 spores per larva. In brief, deceased individuals were collected every other day, placed into 2 mL Eppendorf tubes containing 1 mL of deionized water and a stainless-steel bead (Ø 5 mm), and stored at 4℃. These individuals (approximately 15 per tube) were later homogenized using a Qiagen TissueLyser LT at a frequency of 30 Hz for 2 minutes and then used to infect new larvae.

Experimental evolution and rearing

We performed experimental evolution to create four selection treatments in a fully factorial design: selection for early *vs*. late reproduction, and selection in the absence *vs*. presence of *V. culicis*. Each regime was replicated four times (16 lines total). In every generation of selection and maintenance, we ensured a density of at least 200 adult individuals. To start the experiment, eggs from the stock UGAL colony were hatched synchronously under reduced air pressure and distributed among 16 lines. Each line was maintained separately across ten generations with a standardized density of larvae per generation. Larvae were reared in deionized water (800 ml in a plastic tray) and fed daily with Tetramin Baby ® fish food in the following daily doses: 0.04, 0.053, 0.107, 0.213, 0.64, 0.32 mg/larva for days 1, 2, 3, 4, 5, 6 and later, respectively. At the pupae stage, individuals were transferred to cups (5 cm Ø x 10 cm) placed inside cages (30 x 30 x 30 cm), and adults were provided with *ad libitum* access to 6% sucrose.

For selection lines exposed to the parasite, larvae were exposed to *V. culicis* spores 48 h after hatching by adding 20,000 spores/larva (infective stage) to the water and gently mixing. Naive (control) lines experienced identical handling but received parasite-free water. Spore concentration was assessed using a hemocytometer under a phase-contrast microscope before each infection.

All females received their first blood meal at a fixed age interval post-hatching. Females were fed on human skin (AB's and LMS' arm) for selection and post-selection readouts. In early-reproduction lines, only eggs laid in the first clutch were used to found the next generation. In late-reproduction lines, females received repeated blood meals at fixed intervals, and only eggs from the last clutch (collected when approximately two-thirds of females had died) were used to start the following generation. This design generated four selection treatments: (i) exposed x early; (ii) exposed x late; (iii) naive x early; and (iv) naive x late. Before measuring responses to selection, a generation without any selective pressures was given to avoid parental effects on our post-selection measurements.

Responses to selection

Before assessing any trait, selection was halted for one generation to avoid carry-over effects from parental generations. Longevity and oxidative stress were assessed at generation F12, while fecundity was assessed at F18.

Longevity assay: To quantify evolved differences in lifespan and infection outcomes, we reared larvae from each selection line individually. Eggs from each line were synchronously hatched, and 48-hour-old larvae were transferred and individualized in single wells of 12-well plates, containing 3 mL of deionized water, and fed daily as above. For each line, half of the larvae were infected with *V. culicis* (20,000 spores per larva) and half remained uninfected. Pupae were then transferred individually to small cups enclosed within larger cages, and adults had ad libitum access to 6% sucrose. Mosquitoes were monitored daily until death. Dead individuals were frozen for later assessment of infection status and parasite load by homogenizing whole bodies in deionized water and counting spores with a hemocytometer. These data were used to quantify longevity, infection probability, and parasite burden across selection regimes.

Fecundity assay: To quantify the effect of selection on reproduction, we measured fecundity in all selection lines in a full-factorial design (four selection treatments x four replicate lines x two infection treatments [infected or not]). Freshly emerged larvae (3–6 h old) from each line were reared individually in 24-well plates (one larva per well, 3 mL deionized water per well) and fed daily as described above. Larvae assigned to the infected group were exposed to 20,000 spores in 3 mL of water at 2 days post-hatching. In contrast, uninfected controls received parasite-free water. Pupae were transferred to 180 mL cups within 30 × 30 × 30 cm cages. To control for paternal effects, males emerging from the

selection lines were replaced by stock males at a 1:1 male-to-female ratio. Adults were allowed to mate for seven days in groups of 100 per cage, after which stock males were removed. Females were offered a human blood meal (LMS arm) for 7–8 minutes at three adult ages: 7-, 21-, and 35 days post-emergence. Two days after each blood meal, females were gently transferred to individual oviposition cups (standard 180 mL plastic cups with moist filter paper) and kept there for egg laying. Females were then frozen at −20 °C. We counted the number of eggs per female per time window, and measured wing length as a proxy for body size.

Oxidative stress assay: To measure evolved differences in redox physiology, we quantified oxidative stress markers in uninfected females from three (out of four) randomly selected replicates of each selection treatment. For each line, 120 larvae were hatched under reduced air pressure and reared individually in 12-well plates (3 mL deionized water per well). Pupae were transferred to 180 mL cups for emergence, and adults were kept in 30 x 30 x 30 cm cages with 6% sucrose solution. Females were collected at specific ages (5- and 15-days post-emergence), killed by freezing at −80 °C, and stored individually in 2 mL microcentrifuge tubes. For each mosquito, the wings and legs were removed, and the body was weighed to the nearest 0.01 mg. The body was then homogenized in 120 µL phosphate-buffered saline using a 2 mL tube with a 5 mm stainless-steel bead in a Tissue Lyser (4 min, 45 Hz). Homogenates were centrifuged (10,000 rpm, 10 min, 4 °C), and supernatants were split into aliquots for glutathione (GSH, GSSG), MDA, and SOD assays. GSH and GSSG were extracted and quantified by UHPLC–MS/MS using established protocols [31]. MDA was measured by HPLC–MS against a standard curve prepared from MDA tetrabutylammonium salt, after a phase-partitioning and evaporation step. SOD activity was measured using the Superoxide Dismutase Assay Kit (Cayman Chemical), with mosquito homogenates diluted 1:8 in PBS; samples were run in duplicate and averaged for analysis. There was no difference across selection treatments in either time point, so they were combined in the analyses and figures of the study.

Statistical analyses

All analyses and plots were performed with R version 4.5.2 in RStudio version 2025.09.2+418 using the packages "car", "lme4", "DHARMa", "ggplot2", "dplyr", "tidyr", "emmeans", "multcomp", "scales", "purrr", "mgcv" and "mgcViz". Biorender.com was used to assemble the figure panels. Significance was assessed with the "Anova" function of the "car" package. We used a Type III ANOVA when a significant interaction was present, and a Type II ANOVA otherwise. When relevant, we performed post hoc multiple comparisons using the "emmeans" package with the default Tukey adjustment.

Longevity (median age at death) was analyzed using a linear mixed model (LMM) with reproductive regime (early *vs.* late), parasite exposure during evolution (naïve *vs.* exposed), and their interactions as

fixed effects, and line as a random effect. This was performed separately for each sex **(Supplementary Table 1)**.

Fecundity (egg counts of egg-laying females transformed by a quadratic function) was analyzed using an LMM with reproductive selection, parasite selection, and infection as explanatory variables, as well as their interaction, and replicate as a random factor. A separate LMM was run for each fecundity window **(Supplementary Table 2)**.

Redox markers (GSH, GSSG, GSH: GSSG ratio, MDA, SOD) were also analyzed using LMMs with reproductive regime, parasite exposure during evolution, and their interactions as fixed effects, and line as a random effect. To assess changes in redox physiology across selection treatments, we performed a principal component analysis (PCA) on the means of each line for the five oxidative markers. Before running the PCA, markers were mean-centred and scaled to unit variance. PCA was conducted using the "prcomp" function in R, and loadings were extracted to identify the main axes of variation **(Supplementary Tables 3 and 4)**. We focused on PC1 and PC2 for visualization and assessed separation among selection regimes qualitatively, given the limited number of replicate lines.

To test whether multivariate redox profiles predicted evolved differences in aging, we related PC1 (redox gradient) scores to the median adult longevity of each line. We first fitted a simple linear model with PC1 as a predictor. We then used a generalized additive model (GAM) with a smooth term for PC1 to allow for non-linear relationships (using the "gam" function in the "mgcv" package) **(Supplementary Table 5)**. Model residuals were inspected to confirm assumptions. Given the small number of lines, we interpreted these analyses cautiously, focusing on the direction and shape of the association rather than on precise effect size estimates.

Data availability

All data generated are provided as Supplementary File 2-4

Code availability

The R script used for statistical analyses is provided as Supplementary File 5.

Acknowledgments

We would like to thank Alexei A. Maklakov, Alfonso Rojas-Mora, Tiago G. Zeferino, and Thomas Flatt for their valuable feedback throughout the project. AB, LMS and the project were supported by the SNF grant 310030_192786.

Author contributions

AB and JCK conceived the project. AB, LMS and JCK designed the experiments. AB and LMS conducted the experiments. LMS analyzed the data and wrote the first draft of the manuscript.

Competing interests

All authors declare no financial or non-financial competing interests.

References

1. Williams, G. C. Natural selection, the costs of reproduction, and a refinement of Lack's principle. *Am. Nat.* **100**, 687–690 (1966).

2. Hamilton, W. D. The moulding of senescence by natural selection. *J. Theor. Biol.* **12**, 12–45 (1966).

3. Kirkwood, T. B. L. Evolution of ageing. *Mech. Ageing Dev.* **123**, 737–745 (2002).

4. Charlesworth, B. Evolution in age-structured populations. (1994).

5. Rose, M. R. Antagonistic pleiotropy, dominance, and genetic variation. *Heredity (Edinb).* **48**, 63–78 (1982).

6. Lorenzini, A., Stamato, T. & Sell, C. The disposable soma theory revisited: time as a resource in the theories of aging. *Cell Cycle* **10**, 3853–3856 (2011).

7. Rose, M. R. %J E. Laboratory evolution of postponed senescence in Drosophila melanogaster. **38**, 1004–1010 (1984).

8. Kirkwood, T. B. L. & Rose, M. R. Evolution of senescence: late survival sacrificed for reproduction. *Philos. Trans. R. Soc. London. Ser. B Biol. Sci.* **332**, 15–24 (1991).

9. Fabian, D. K. *et al.* Evolution of longevity improves immunity in Drosophila. *Evol. Lett.* (2018).

10. Slade, L., Etheridge, T. & Szewczyk, N. J. Consolidating multiple evolutionary theories of ageing suggests a need for new approaches to study genetic contributions to ageing decline. *Ageing Res. Rev.* **100**, 102456 (2024).

11. Aronoff, J. E. & Trumble, B. C. An evolutionary medicine and life history perspective on

aging and disease: Trade-offs, hyperfunction, and mismatch. *Evol. Med. Public Heal.* **13**, 111–124 (2025).

12. Harman, D. Free radical theory of aging: history. *Free radicals aging* 1–10 (1992).

13. Silva, L. M. The transcriptome of the mosquito host Anopheles gambiae upon infection by different selected lines of the microsporidian parasite Vavraia culicis. *bioRxiv* 2009–2024 (2024). doi:https://doi.org/10.1101/2024.09.22.613703

14. Silva, L. M. & Koella, J. C. Complex interactions in the life cycle of a simple parasite shape the evolution of virulence. *PLoS Pathog.* (2025). doi:https://doi.org/10.1371/journal.ppat.1013294

15. Zeferino, T. G., Rojas Mora, A., Vallat, A. & Koella, J. C. Dietary shifts in infected mosquitoes suggest a form of self-medication despite benefits in uninfected individuals. *Proc. B* **292**, 20251659 (2025).

16. Graham, A. L., Allen, J. E. & Read, A. F. Evolutionary causes and consequences of immunopathology. *Annu. Rev. Ecol. Evol. Syst.* **36**, 373–397 (2005).

17. Baylis, D., Bartlett, D. B., Patel, H. P. & Roberts, H. C. Understanding how we age: insights into inflammaging. *Longev. Heal.* **2**, 8 (2013).

18. Schneider, D. S. & Ayres, J. S. Two ways to survive infection: what resistance and tolerance can teach us about treating infectious diseases. *Nat. Rev. Immunol.* **8**, 889 (2008).

19. Silva, L. M., Zeferino, T. G. & Koella, J. C. Vavraia culicis. *Trends Parasitol.* (2025). doi:https://doi.org/10.1016/j.pt.2025.02.011

20. Stearns, S. C. *The evolution of life histories*. **249**, (Oxford university press Oxford, 1992).

21. Crews, D. E. & Bogin, B. Growth, development, senescence, and aging: a life history perspective. *A companion to Biol. Anthropol.* 124–152 (2010).

22. Speakman, J. R. & Selman, C. The free-radical damage theory: accumulating evidence against a simple link of oxidative stress to ageing and lifespan. *Bioessays* **33**, 255–259 (2011).

23. Schieber, M. & Chandel, N. S. ROS function in redox signaling and oxidative stress. *Curr. Biol.* **24**, R453–R462 (2014).

24. Quiros-Roldan, E., Sottini, A., Natali, P. G. & Imberti, L. The impact of immune system aging on infectious diseases. *Microorganisms* **12**, 775 (2024).

25. Zeller, M. & Koella, J. C. The Role of the Environment in the Evolution of Tolerance and Resistance to a Pathogen. *Am. Nat.* **190**, 389–397 (2017).

26. Akyaw, P. A., Paulo, T. F., Lafuente, E. & Sucena, É. Pathogen-induced damage in Drosophila: uncoupling disease tolerance from resistance. *PLoS Pathog.* **21**, e1013482 (2025).

27. Zeferino, T. G. & Koella, J. C. Host-specific effects of a generalist parasite of mosquitoes. *Sci. Rep.* **14**, 18365 (2024).

28. Desjardins, C. A. *et al.* Contrasting host–pathogen interactions and genome evolution in two generalist and specialist microsporidian pathogens of mosquitoes. *Nat. Commun.* **6**, 7121 (2015).

29. López-Otín, C., Blasco, M. A., Partridge, L., Serrano, M. & Kroemer, G. Hallmarks of aging: An expanding universe. *Cell* **186**, 243–278 (2023).

30. Silva, L. M., King, K. C. & Koella, J. C. Dissecting transmission to understand parasite evolution. *PLoS Pathog.* **21**, e1012964 (2025).

31. Mora, A. R., Firth, A., Blareau, S., Vallat, A. & Helfenstein, F. Oxidative stress affects sperm performance and ejaculate redox status in subordinate house sparrows. *J. Exp. Biol.* **220**, 2577–2588 (2017).

Supplementary File 1:

Supplementary tables and figures for "Testing the redox theory of aging under parasitism"

by Luís M. Silva *, Alessandro Belli * and Jacob C. Koella

*These authors contributed equally to this study.

This document includes the following:

Supplementary Table 1. Longevity and fecundity after selection.
Supplementary Table 2. MDA concentration across selection treatments.
Supplementary Table 3. Summary of the principal component analysis.
Supplementary Table 4. Loadings of oxidative markers on PCA.
Supplementary Table 5. Relationship between oxidative PCA axis and longevity.

Supplementary Figure 1. Design of the experimental evolution setup.
Supplementary Figure 2. Post selection measurements: parasite load at death.
Supplementary Figure 3. Post selection measurements: oxidative markers.

Tables

Supplementary Table 1. Longevity and fecundity after selection. After selecting for early or late reproduction, regardless of exposure to parasitism or not, we measured longevity and fecundity throughout the mosquito's life. First, we assessed changes in longevity in the absence of infection across selection treatments for male and female mosquitoes, separately. We used a linear mixed model with the two forms of selection (reproduction and exposure to parasitism) as explanatory variables in interaction and replicate as a random factor. For fecundity, we assessed each window separately and quantified the number of eggs laid at 7, 21 and 35 days of adult age. For the best model fit, the number of eggs was transformed using a quadratic function. Using linear models similar to those for longevity, we quantified the cost of selection on reproductive life output.

Tested effect

Model 1a: Female longevity after selection	***χ2***	***df***	***p***
Selection reproduction	20.62	1	**< 0.001**
Selection parasitism	8.07	1	**0.005**
Selection reproduction : Selection parasitism	2.09	1	0.148
Multiple comparisons for Model 1a	**estimate**	***t***	***p***
Exposed x Early *vs* Naive x Early	84.8	0.98	0.762
Exposed x Early *vs* Exposed x Late	-362.7	-4.25	**0.013**
Exposed x Early *vs* Naive x Late	-101.8	-1.19	0.652
Naive x Early *vs* Exposed x Late	-447.6	-5.17	**0.004**
Naive x Early *vs* Naive x Late	-186.6	-2.15	0.216
Exposed x Late *vs* Naive x Early	261.0	3.03	0.064
Model 1b: Male longevity after selection	***χ2***	***df***	***p***
Selection reproduction	1.29	1	0.260
Selection parasitism	4.23	1	**0.040**
Selection reproduction: Selection parasitism	0.11	1	0.738
Model 1cd: Day 7 fecundity	***χ2***	***df***	***p***
Selection parasitism	13.10	1	**< 0.001**
Selection reproduction	0.34	1	0.560
Infection treatment	0.44	1	0.508
Selection parasitism : Selection reproduction	8.01	1	**0.005**
Selection parasitism : Infection treatment	3.70	1	0.052
Selection reproduction : Infection treatment	0.35	1	0.556
Multiple comparisons for Model 1cd: selection	**estimate**	***t***	***p***
Exposed x Early *vs* Naive x Early	6.60	3.14	**0.010**

Exposed x Early *vs* Exposed x Late	-0.61	-0.29	0.991
Exposed x Early *vs* Naive x Late	-2.49	-1.17	0.644
Naive x Early *vs* Exposed x Late	-7.21	-3.39	**0.004**
Naive x Early *vs* Naive x Late	-9.09	-4.18	**< 0.001**
Exposed x Late *vs* Naive x Early	-1.89	-0.88	0.816
Model 1cd: Day 21 fecundity	***χ2***	***df***	***p***
Selection parasitism	0.11	1	0.741
Selection reproduction	5.84	1	**0.016**
Infection treatment	27.95	1	**< 0.001**
Selection parasitism : Selection reproduction	0.01	1	0.960
Selection parasitism : Infection treatment	0.81	1	0.368
Selection reproduction : Infection treatment	0.53	1	0.465
Model 1cd: Day 35 fecundity	***χ2***	***df***	***p***
Selection parasitism	18.40	1	**< 0.001**
Selection reproduction	5.43	1	**0.020**
Infection treatment	0.03	1	0.871
Selection parasitism : Selection reproduction	3.58	1	0.059
Selection parasitism : Infection treatment	2.27	1	1.132
Selection reproduction : Infection treatment	1.75	1	0.185

Supplementary Table 2. MDA concentration across selection treatments. We quantified oxidative damage by measuring malondialdehyde (MDA) concentration in adult female mosquitoes originating from lines selected for early or late reproduction, with or without exposure to parasitism. A linear model with reproduction- and parasite-selection as interacting fixed effects was used to test for differences in MDA levels. Shown are the Type II Wald χ^2 statistics, degrees of freedom, and *p*-values for each fixed effect in Model 2a.

Tested effect			
Model 2a	***χ2***	***df***	***p***
Selection reproduction	1.33	1	0.248
Selection parasitism	5.16	1	**0.023**
Selection reproduction : Selection parasitism	4.63	1	**0.031**

Supplementary Table 3. Summary of the principal component analysis. PCA variance in the presented Figure 2b (underlined values). Eigenvalues, proportion of variance, and cumulative variance explained by the first principal components describing variation in oxidative stress markers across selection lines. These axes were used to summarise the multivariate redox gradient among lines selected for early or late reproduction, with or without exposure to parasitism.

	Eigenvalue	Proportion of variance	Cumulative variance
PC1	1.955	0.391	0.391
PC2	1.659	0.332	0.723
PC3	1.025	0.204	0.927
PC4	0.236	0.047	0.975
PC5	0.125	0.025	1.000

Supplementary Table 4. Loadings of oxidative markers on PCA. Loadings of mean GSH, GSSG, redox ratio, MDA, and SOD concentrations on the first two principal components from the PCA of oxidative markers. Positive and negative values indicate the direction and strength of each trait's contribution to the multivariate redox gradient separating selection treatments.

Trait	Loading PC1	Loading PC2
GSH/GSSG ratio	0.634	-0.281
GSSG	0.535	-0.418
GSH	-0.455	-0.499
SOD	-0.308	-0.652
MDA	0.096	-0.268

Supplementary Table 5. Relationship between oxidative PCA axis and longevity. Linear (LM) and generalized additive (GAM) models relating median adult longevity (uninfected assay) to PC1 scores from the PCA of oxidative markers (**Figure 2b,c; Supplementary Tables 3 and 4)**. For the LM, slope estimate, standard error, t-value, p-value, R^2 and adjusted R^2 are shown. For the GAM, effective and reference degrees of freedom (edf, ref. df), F-value, p-value, R^2 and explained deviance are shown. Negative slopes indicate that lines with more oxidized redox profiles (higher PC1 scores) tend to have reduced median lifespan.

	estimate	**std. error**	***t*-value**	***p*-value**	**R^2**	**Adjusted R^2**
PC1 (LM)	-0.876	0.404	-2.168	0.055	0.320	0.252
	edf	**ref. df**	***F*-value**	***p*-value**	**R^2**	**Explained dev.**
PC1 (GAM)	2.18	2.68	5.00	**0.025**	0.551	0.64

Figures

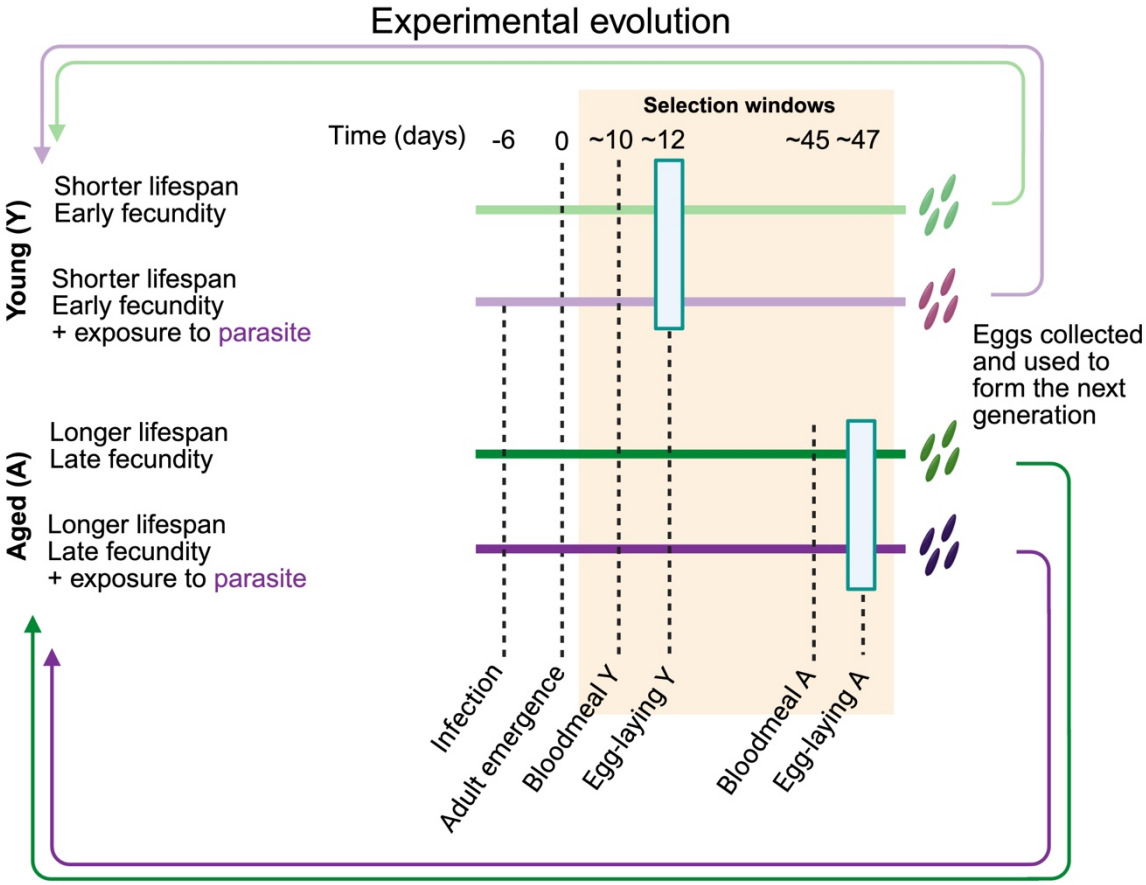

Supplementary Figure 1. Design of the experimental evolution setup. Illustration of the experimental evolution assay. From a single starting stock population of *Aedes aegypti*, four selection treatments were created: (i) Exposed to parasite x Early reproduction; (ii) Exposed to parasite x Late reproduction; (iii) Naive x Early reproduction; and (iv) Naive x Late reproduction. Each selection treatment is composed of four replicate lines run in parallel. Lines selected for early reproduction had the offspring from the first blood meal selected to start the next generation. In contrast, the late-reproduction lines were blood-fed weekly, and the selected clutch of eggs was the result of the blood meal around 45 days after adulthood (when approximately two-thirds of the population had died). Lines exposed to the parasite *V. culicis* were subjected to an infective dose of 20,000 spores per larva, 2 days after eggs had hatched. This was repeated for at least ten generations before measuring all the traits.

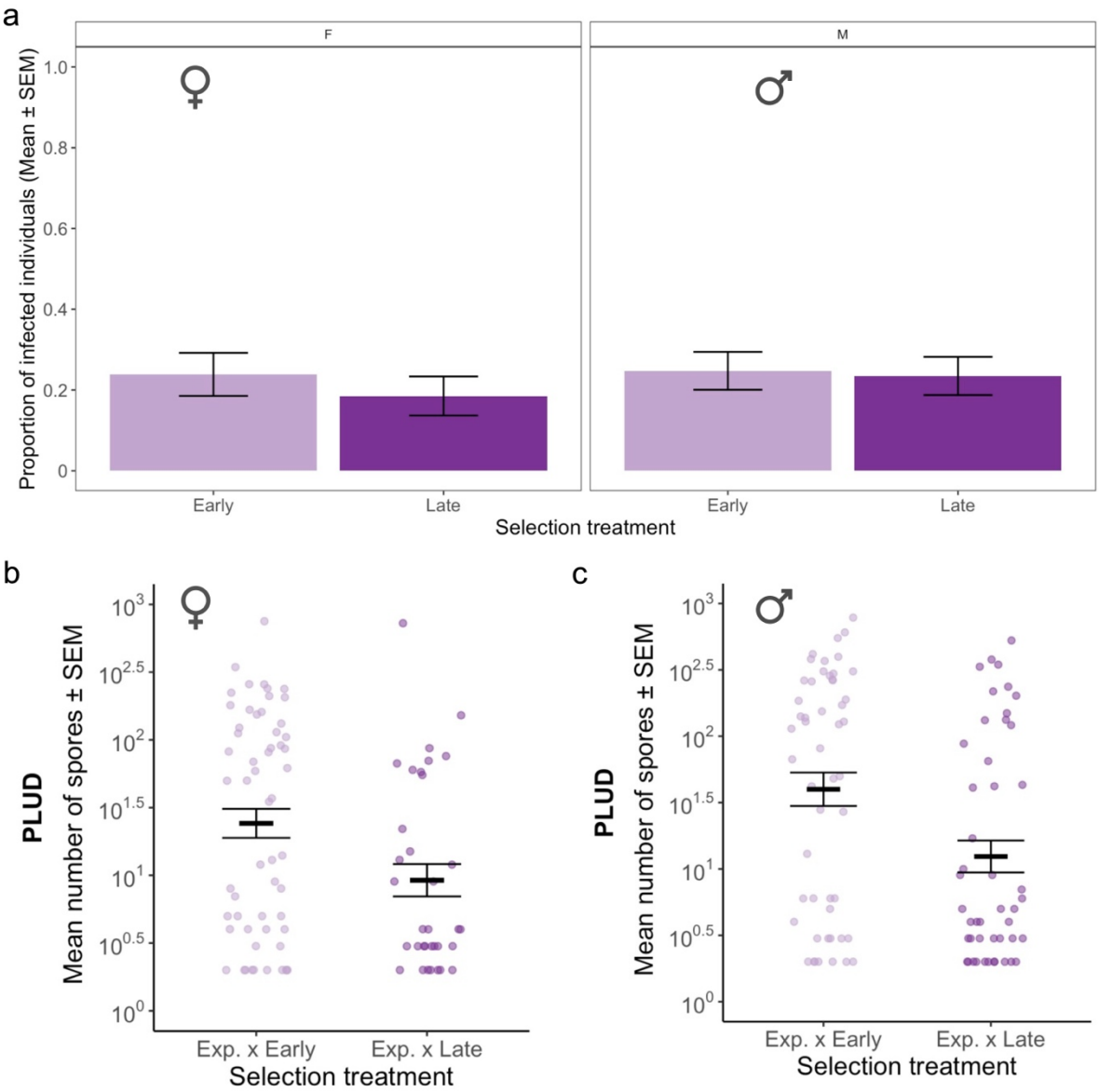

Supplementary Figure 2. Post selection measurements: parasite load at death. As individuals died during the longevity assay, they were collected to quantify **(a)** the proportion of infected females and males. From those who did not clear infection, the mean number of spores was counted and compared for **(b)** females, and **(c)** males. No statistical difference was found between treatments for any of the comparisons.

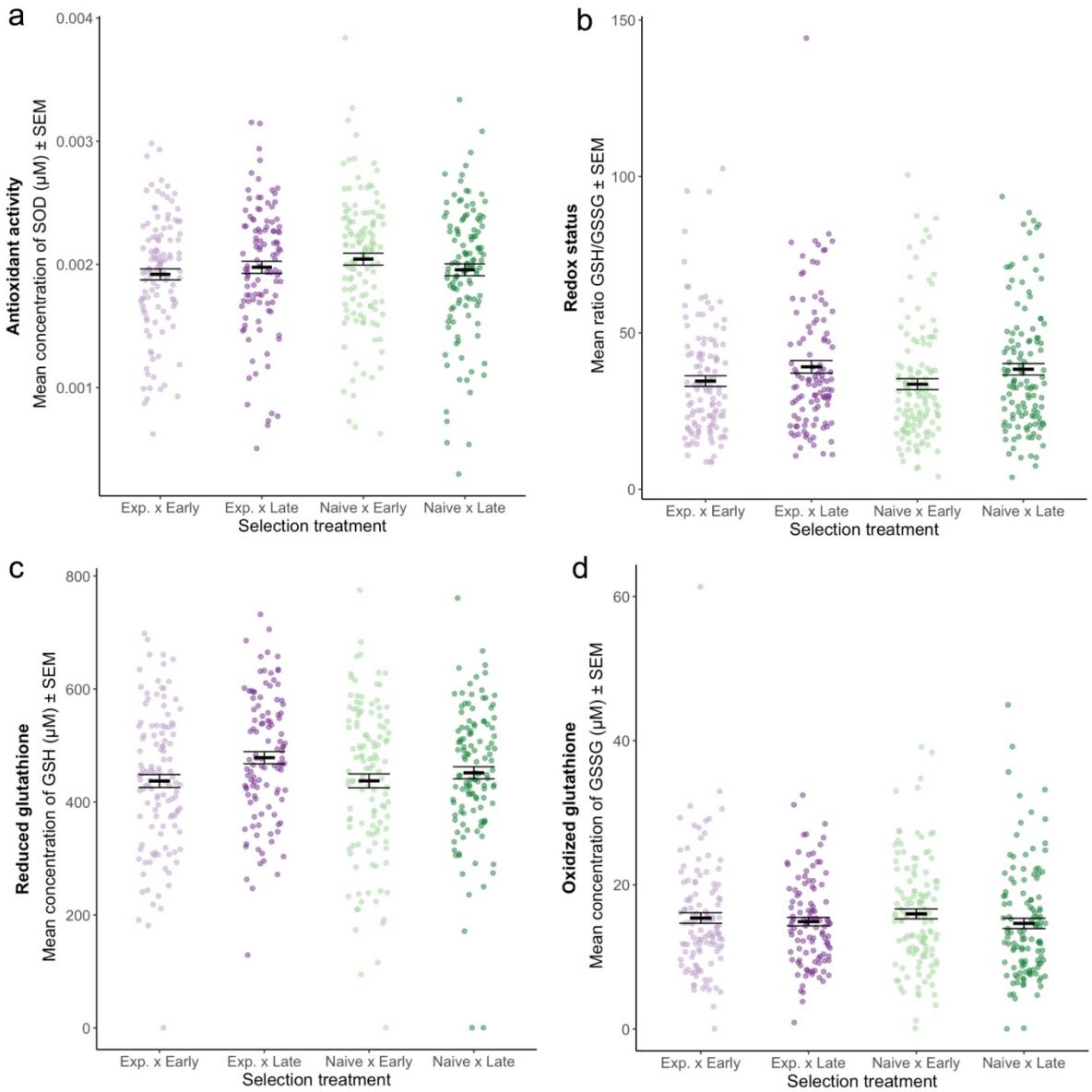

Supplementary Figure 3. Post selection measurements: oxidative markers. Mean concentrations, and respective errors, of **(a)** superoxide dismutase (SOD, marker of antioxidant activity), **(b)** the GSH: GSSG ratio (proxy for redox status), **(c)** reduced glutathione (GSH), and **(d)** oxidized glutathione (GSSG) measured in uninfected females from each selection treatment at day 5 and 15 of age. There was no difference across selection treatments in either time point, so they were combined. None of the markers showed any difference across selection treatments.